

Preparation of V-Fe Gradient Materials on Carbon Steel by Electrodeposition in a NaCl-KCl-NaF-V₂O₃ Molten Salt

Changqing Li, Jiantao Liu, Mingyu Wu, Ying Tian, Haichao Zhang, Yungang Li*

Key Laboratory of Ministry of Education for Modern Metallurgy Technology, College of Metallurgy and Energy, North China University of Science and Technology, 21# Bohai Road, Caofeidian Xincheng, Tangshan 063210, China

*E-mail: liyungang59322@163.com

Received: 3 April 2020 / Accepted: 2 June 2020 / Published: 10 July 2020

The electrochemical reduction mechanism of V₂O₃ was analyzed by cyclic voltammetry and chronopotentiometry in a NaCl-KCl-NaF molten salt at 973K. Chronoamperometry was used to investigate the electrocrystallization process of vanadium. The electrochemical reduction of V₂O₃ is a quasi-reversible process mix-controlled by the V³⁺ diffusion rate and the electron transport rate; the reduction mechanism of V₂O₃ in the molten salt is a one-step process, V³⁺ + 3e⁻ → V, where the diffusion coefficient of V³⁺ is 1.03×10⁻⁴; the electrocrystallization of V proceeds via an instantaneous hemispheroid three-dimensional nucleation process. A V-Fe gradient material was successfully prepared on a carbon steel substrate. The surface and local morphologies of the coating were analyzed by scanning electron microscopy and energy dispersive spectrometry. Glow discharge spectrometry was used to analyze the cross-section of the V-Fe gradient material coating under experimental conditions. The coating thickness is approximately 5 μm, and the vanadium and iron concentrations exhibit a gradient distribution.

Keywords: Molten salt; electrocrystallization process; V-Fe gradient material; coating

1. INTRODUCTION

Vanadium is a rare metal with strategic importance worldwide. This metal is widely used in aerospace applications, nuclear reactors and other cutting-edge fields[1]. Vanadium is a very important alloying element for iron and steel. Vanadium mainly exists in alloys as compounds and solid solutions[2]. Vanadium can refine the structure and grain of steel, improves the strength and toughness of steel, plays a role in reducing the hardenability of steel during heat treatment of alloy steels, including heat-resistant steel, spring steel, stainless steel, bearing steel and mold steel[3]; at the same time, vanadium can also improve the corrosion resistance of steel materials. Two methods are mainly used to prepare vanadium alloys. The first method involves the direct addition of pure metal vanadium or vanadium oxide to molten metal. The second method involves powder metallurgy.

These two methods are mainly used to prepare high-temperature resistant alloys. The density of the material prepared by the infiltration method is relatively high, but the difficulty of controlling the composition results in an uneven pore distribution that significantly impacts the material performance[4-5]. The powder metallurgy method requires simple equipment, is low cost, and can be used for large-scale production, but the preparation process is complex, and very strict requirements are placed on the temperature, time and cooling speed[6]; however, the aforementioned shortcomings can be circumvented using molten salt electrodeposition, wherein V-Fe gradient materials are prepared by deposition and mutual diffusion. In the phase diagram of a V-Fe binary alloy, both vanadium and iron have body-centred cubic lattices for a 0-24% vanadium content over a 973-1073K temperature range. Over this temperature range, Fe and V easily form a solid solution alloy, which facilitates the preparation of V-Fe gradient materials. NaCl-KCl-NaF is the system most commonly used to prepare gradient materials by molten salt electrodeposition[7-10]. Mixing chloride and fluoride into this molten salt system can effectively improve the current efficiency and production capacity.

In this study, a method for preparing V-Fe gradient materials was proposed using a NaCl-KCl-NaF-V₂O₃ molten salt system. The electrochemical reduction process of V₂O₃ in the molten salt system and the mechanism of crystallization nucleation were studied. V-Fe gradient materials were prepared by molten salt electrodeposition.

2. EXPERIMENTS

2.1 Materials and Preparation of molten salt

The following materials were used in this study: NaCl, KCl, NaF, V₂O₃, 30 mm ×20 mm×1 mm carbon steel sheets and a zirconia crucible. As adsorbed water in the reagents can enter the molten salt and affect the experimental results, the adsorbed water was completely removed by drying the salt used for 8 hours at 393K before beginning the experiment; the dried salt was then ground and sealed to use as needed.

2.2 Selection and preparation of electrode

A three-electrode system, including working, reference, and counter electrodes, was used to investigate the mechanism of the electrochemical reaction. The working and reference electrodes were both high-purity Pt wire, and graphite was used as the counter electrode. The cathode was pretreated before beginning the experiment. The specific process consisted of mechanical pretreatment, oil removal and cleaning.

(1) Mechanical pretreatment

The electrode surface was first sanded with silicon carbide sandpaper (150 and 800 mesh), followed by light sanding with metallographic sandpaper (1 and 3 mesh) until a mirror surface appeared.

(2) Degreasing

As oil on a substrate directly affects the quality of a deposition layer and pollutes the electrolyte, oil was removed from the substrate surface. A chemical method was used, where the electrode was placed in a 5% NaOH solution for 10min.

(3) Cleaning

The electrode was first washed using deionized water in an ultrasonic cleaner for 5min and then washed with alcohol and dried to be used as needed.

2.3 Experimental devices

The experimental equipment consists of a high-temperature resistance furnace for heating, an artificial intelligence regulator (AI-808p type) for temperature control, a platinum-platinum rhodium thermocouple for temperature measurement, and a smart multi-group commutation pulse plating power source, imported from Germany, for electrodeposition. An IM6eX-type electrochemical measurement system (under microcomputer control) is used to study the electrochemical mechanism.

2.4 Experimental procedure

The raw materials were weighed and mixed in specific proportions (i.e. $X_{\text{NaCl}} = 0.4$; $X_{\text{KCl}} = 0.4$; $X_{\text{NaF}} = 0.2$; and $X_{\text{V}_2\text{O}_3} = 0.01$), filled into a high-purity graphite crucible, covered with a graphite lid, and placed in a heating furnace through which argon was passed. To prevent oxidation of the graphite crucible and the electrode, a platinum-platinum rhodium thermocouple was inserted into a stainless steel sleeve, and the temperature was increased to 973 K at a controlled rate of $10 \text{ K} \cdot \text{min}^{-1}$. After stabilization of the furnace temperature, and the working and reference electrodes were inserted. The IM6eX-type electrochemical measurement system was connected, and the three-electrode system was used to investigate the electrochemical mechanism. The aforementioned molten salt system was used to conduct an electrodeposition experiment with carbon steel as the cathode at 973 K for a current density of $200 \text{ mA} \cdot \text{cm}^{-2}$ and an electrodeposition time of 60 minutes.

2.3 Detection and analysis

The composition of the molten salt system was determined using a X-ray diffractometer (XRD, Empyrean of PANalytical B.V.) at a scan speed of 5° min^{-1} over a 2θ range from 10° to 90° . The surface morphology and chemical composition of the deposited samples were analyzed using a scanning electron microscope and an energy dispersive spectrum analyzer (SEM-EDS, Shimadzu, Japan). The sample cross section was analyzed using an optical microscope and a field emission scanning electron microscope. The elemental content of the sample cross section was measured as a function of the sample depth using a GDA750 glow discharge spectrometer.

3. RESULTS AND DISCUSSION

3.1 Cyclic voltammetry

The molten salt system (composition: $X_{\text{NaCl}} = 0.4$; $X_{\text{KCl}} = 0.4$; $X_{\text{NaF}} = 0.2$; and $X_{\text{V}_2\text{O}_3} = 0.01$) was used to investigate the electrochemical reduction mechanism of vanadium. The experimentally measured cyclic voltammetry curve is shown in Fig. 1.

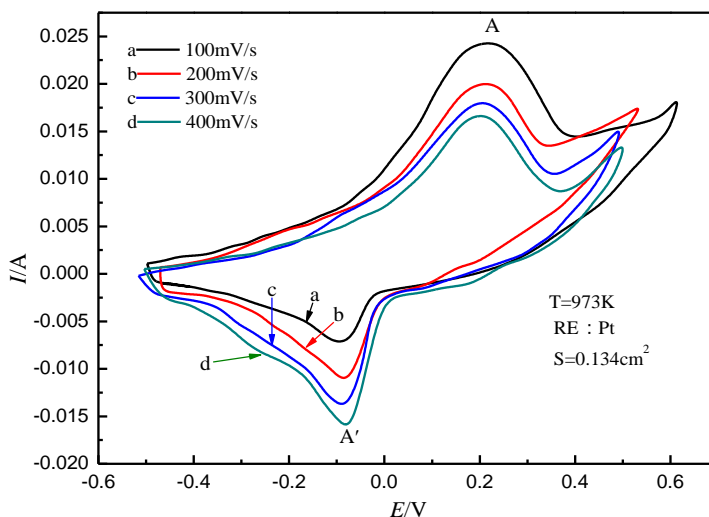


Figure 1. Typical CV curves for electrochemical reaction in a molten salt system at different scan rates with Pt as the working electrode at 973 K

Figure 1 shows the cyclic voltammetry curve of the NaCl-KCl-NaF-V₂O₃ molten salt system at 973 K. A cathodic reduction peak A' and an anodic oxidation peak A can be observed at different scan speeds. The reduction potential is approximately -0.094 V (which corresponds to the Pt electrode potential at the reaction temperature), and the oxidation peak potential is approximately 0.2 V. In the diagram, the oxidation and reduction peaks become increasingly defined as the scan rate increases, and E_{pc} and E_{pa} shift to negative and positive potentials as v increases; this result is obtained because the peak current is proportional to the scan rate, and the peak shift is related to the polarization. The large scan rate and polarization result in the positive and negative shifts of the oxidation and reduction peak potentials, respectively, and the current density i_{pc} increases with the scan rate, where a plot of i_{pc} vs. $v^{1/2}$ is shown in figure 2. This relationship is clearly nonlinear. Therefore, the reduction process corresponding to the cathodic reduction peak A' is a simple electrode process that accords with the criterion of a quasi-reversible electrode process. The diagram also shows that $i_{\text{pa}}/i_{\text{pc}} > 1$, that is, $|i_{\text{pa}}/i_{\text{pc}}| > 1$ [11], which shows that the product obtained at the cathode is insoluble. Therefore, the cathodic reduction reaction of V₂O₃ in this system is mix-controlled by the V³⁺ diffusion rate and the electron transport rate, and the product is insoluble. This result is consistent with that of Li et al. [12] for the electrochemical reduction of WO₃ in a NaCl-KCl-NaF-WO₃ molten salt, which is also mix-

controlled by the diffusion rate and the electron transport rate.

The experimental NaCl-KCl-NaF-V₂O₃ molten salt system was analyzed by X-ray diffraction; the results in Fig. 3 show that the vanadium ion in the NaCl-KCl-NaF-V₂O₃ system mainly exists in the V³⁺ form, such that the electrode reaction corresponding to the cathodic reduction peak A' in Fig. 1 is given by $V^{3+} + 3e^- \rightarrow V$.

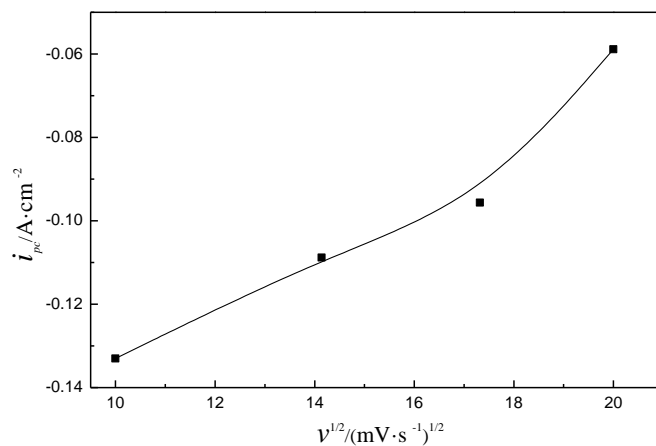


Figure 2. Relationship between i_{pc} and $v^{1/2}$ for reduction peak A' in cyclic voltammogram at 973K

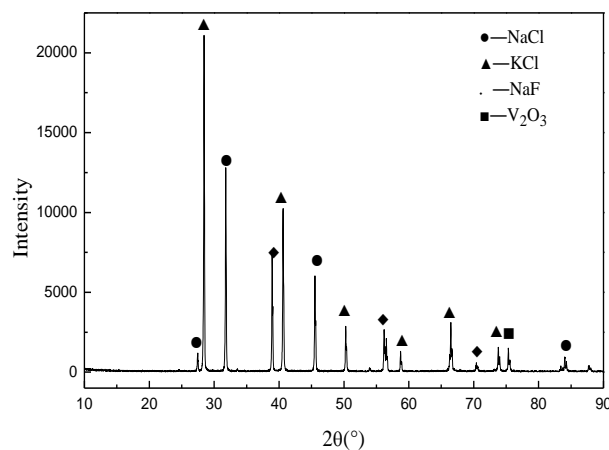


Figure 3. XRD spectrum of NaCl-KCl-NaF-V₂O₃ molten salt system under experimental conditions

3.2 Chronopotentiometry

When the temperature of the molten salt system is 973 K, a large constant current is suddenly applied, and the change of the electrode potential with time is recorded. The obtained chronopotentiometry curve is shown in Fig. 4. The moment at which the constant current is suddenly applied to the system causes ohmic polarization of the solution at the electrode surface, which produces a large change in the electrode potential of the system, as shown by the curve o ~ a. The

polarization of the current reduces the electroactive vanadium ions at the electrode surface to metal vanadium at a constant rate, and the electrode potential accordingly reaches the characteristic value of the electrode reaction (point b). The continuous precipitation of vanadium on the electrode causes the ratio of the V^{3+} concentration at the electrode surface to the precipitated vanadium concentration to change with time. When the ratio is close to 1, the change in the potential tends to be stable, because there is a small change in an electric quantity in unit time, corresponding to the b~c period in the curve; as the electrolysis process continues, the electrode surface concentration polarization starts to dominate, which is accompanied by a significant change in the electrode potential, as shown in the c~d period of the curve. When the reactant concentration at the electrode surface drops to zero (point d), the reactant mass reaching the electrode surface in unit time cannot meet the requirements of the external current. At this time, the electrode potential changes significantly and rapidly until a new reduction process at the electrode begins[13].

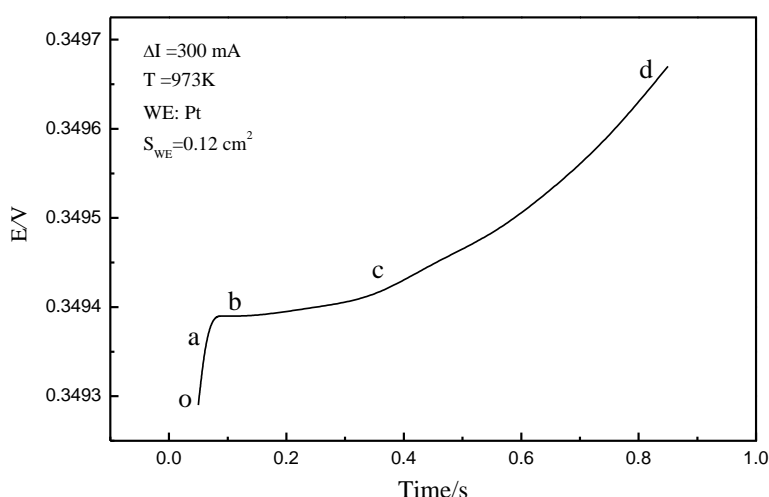


Figure 4. Chronopotentiometry curve of NaCl-KCl-NaF-V₂O₃ molten salt system for 300-mA constant current and Pt as working electrode at 973K

Fig. 5 shows E vs. $\ln(\tau^{1/2}-t^{1/2})$ (where τ is the transition time). Depending on whether the reduction process of V_2O_3 at the cathode is reversible or irreversible, E vs. $\ln(\tau^{1/2}-t^{1/2})$ satisfies equation (1) or equation (2), respectively.

When the reduction process is reversible, and the product is insoluble,

$$E = E_{\tau/4} + \frac{RT}{nF} \ln(\tau^{1/2} - t^{1/2}) \tag{1}$$

When the reduction process is completely reversible,

$$E = E^0 + \left(\frac{RT}{an_a F}\right) \ln\left(\frac{2k^0}{\sqrt{D_0\pi}}\right) + \left(\frac{RT}{an_a F}\right) \ln(\tau^{1/2} - t^{1/2}) \tag{2}$$

Thus, E vs. $\ln(\tau^{1/2}-t^{1/2})$ is linear in both cases; however, as figure 5 shows that E changes nonlinearly with $\ln(\tau^{1/2}-t^{1/2})$, it can be inferred that the reduction of V_2O_3 at the cathode is neither reversible nor irreversible, but quasi-reversible. This inference is consistent with the conclusion obtained by cyclic voltammetry.

The equations given in [14] can be used to derive a relationship between the diffusion coefficient D and the transition time t of the electroactive ions in solution:

$$D = \frac{\tau \cdot 2^2 \cdot i^2}{n^2 \cdot F^2 \cdot \pi \cdot C^2} \tag{3}$$

where τ is the transition time (s), C is the concentration of electroactive particles (mol/cm^3), i is the current density (A/cm^2), n is the number of electrons transferred, and F is the Faraday constant ($\text{C}\cdot\text{mol}^{-1}$).

The diffusion coefficient D of the electroactive V^{3+} ions calculated using Eq. (3) is shown in Table 1. The V^{3+} diffusion coefficient in the NaCl-KCl-NaF- V_2O_3 molten salt is 3.04×10^{-4} at 973 K.

Table 1. Electrochemical parameters of a chronopotentiogram with a 300 mA constant current and Pt as the working electrode at 973 K

I/A	$i/\text{A}\cdot\text{cm}^{-2}$	τ/s	$D/\text{cm}^2\cdot\text{s}^{-1}$	$\bar{D}/\text{cm}^2\cdot\text{s}^{-1}$
0.70	5.833	1.13	5.62×10^{-4}	
0.50	4.167	1.02	2.59×10^{-4}	3.04×10^{-4}
0.30	2.500	0.85	0.91×10^{-4}	

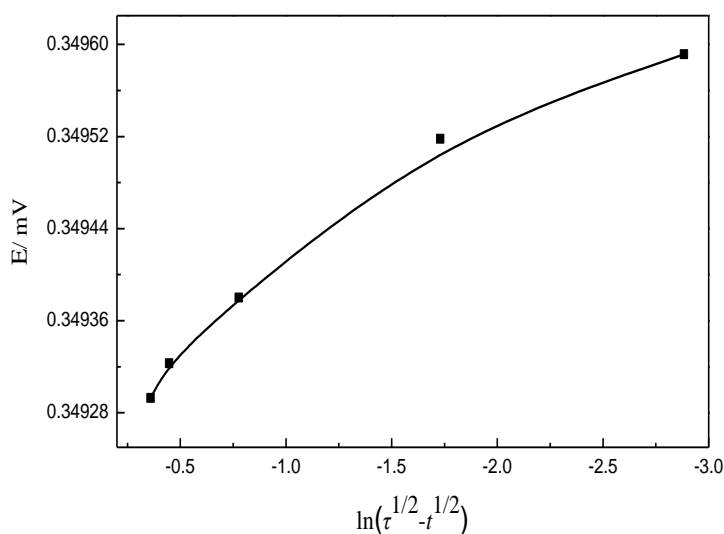


Figure 5. Relationship between E and $\ln(\tau^{1/2}-t^{1/2})$ for reduction peak A' in a chronopotentiogram for a 300 mA constant current

3.3 Chronoamperometry

Fig. 1 shows the chronoamperometry curve for the NaCl-KCl-NaF-V₂O₃ molten salt system at 973 K. Considering the 900 mV curve in figure 6 as an example, the application of the respective voltage to the working electrode creates a circular electric field near the electrode, and the anions and cations in the molten salt migrate directionally under the action of the electric field force. The migration of V³⁺, Na⁺ and K⁺ to the working electrode decreases the difference in the concentration of anions and cations between the working electrode and the reference electrode. Electron transfer to V³⁺ results in the precipitation of V at the surface of the working electrode, which reduces the V³⁺ concentration near the working electrode, increases the resistance of the molten salt and rapidly decreases the current corresponding to 900 mV from 0.025 A to 0.010 A in the chronoamperometry curve. At the same time, V³⁺ enrichment at the surface of the working electrode creates a V³⁺ concentration difference between the working electrode and the molten salt system. Under the action of the concentration gradient and the electric field force, V³⁺ diffuses from the molten salt to the working electrode. As the migration rate of electrons in the conductor is higher than the diffusion rate of the ions in the molten salt, the reaction at the electrode surface is controlled by the diffusion of V³⁺ from the molten salt to the electrode surface. After a period of time, the electron transfer rate and the ion diffusion rate reach a dynamic equilibrium, corresponding to the current stabilization stage at 900 mV in the chronoamperometry curve [15]. Considering the chronoamperometry curves for different voltages in figure 6 leads to the conclusion increasing the applied voltage from 700 mV to 900 mV causes the current at the highest point to increase from 0.020 A to 0.026 A, thereby increasing the polarization of the electrode.

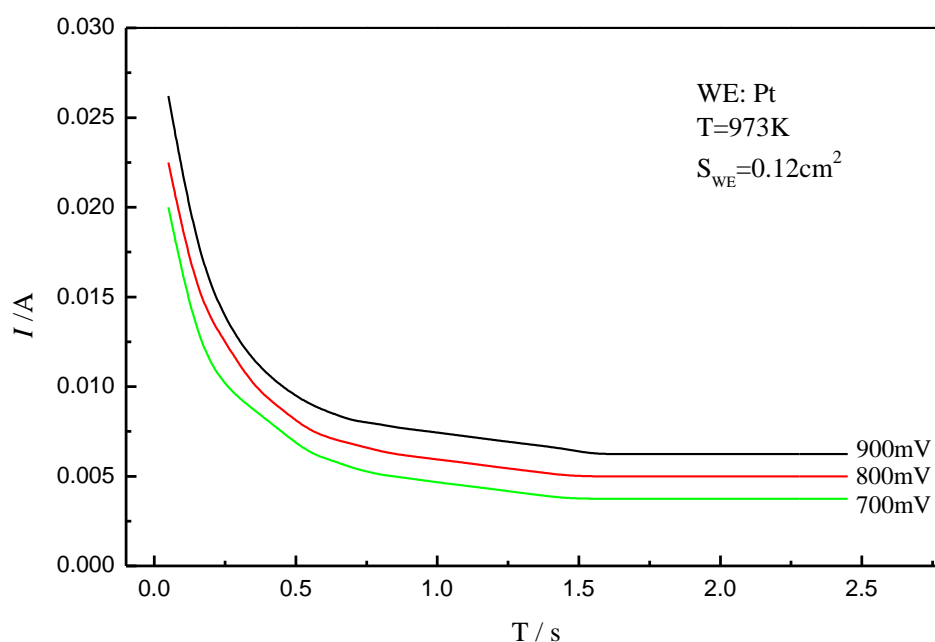


Figure 6. Chronoamperometry curve of electrochemical reduction of V₂O₃ with Pt as working electrode at 973 K

Considering the 900 mV chronoamperometry in Fig. 6 as an example, the extracted I and t data are plotted as I vs. $t^{1/2}$ and I vs. $t^{3/2}$ curves [16] in Fig. 7.

When the electrocrystallization of metal atoms is controlled by diffusion, the relationship between the current and the time is given by the following equations [17-18]:

$$\text{Instantaneous nucleation: } I = nFN\pi(2DC)^{3/2}(M/\rho)^{1/2}t^{1/2} \quad (4)$$

$$\text{Progressive nucleation: } I = \frac{2}{3}nFN\pi K_n(2DC)^{3/2}(M/\rho)^{1/2}t^{3/2} \quad (5),$$

where n is the number of electrons transferred; F is the Faraday constant; N is the maximum density of the crystal nucleus; D is the diffusion coefficient of ions; C is the ion concentration; M is the weight of the electrodeposited atom; and ρ is the density of the electrodeposited substance.

According to three-dimensional nucleation theory, metal nucleation occurs instantaneously, according to the I - $t^{1/2}$ relationship in equation (4), whereas progressive metal nucleation occurs when I varies with $t^{3/2}$ according to equation (5). Figure 7 shows stronger linearity and a higher correlation coefficient R^2 for I vs. $t^{1/2}$ than for I vs. $t^{3/2}$.

It can be concluded that the electric crystallization process of V in the NaCl-KCl-NaF-V₂O₃ system follows an instantaneous hemispheroid three-dimensional nucleation process. This same electric crystallization nucleation process occurs for Ti and Cr in the NaCl-KCl-NaF-TiO₂ and NaCl-KCl-NaF-Cr₂O₃ molten salt systems, respectively[19].

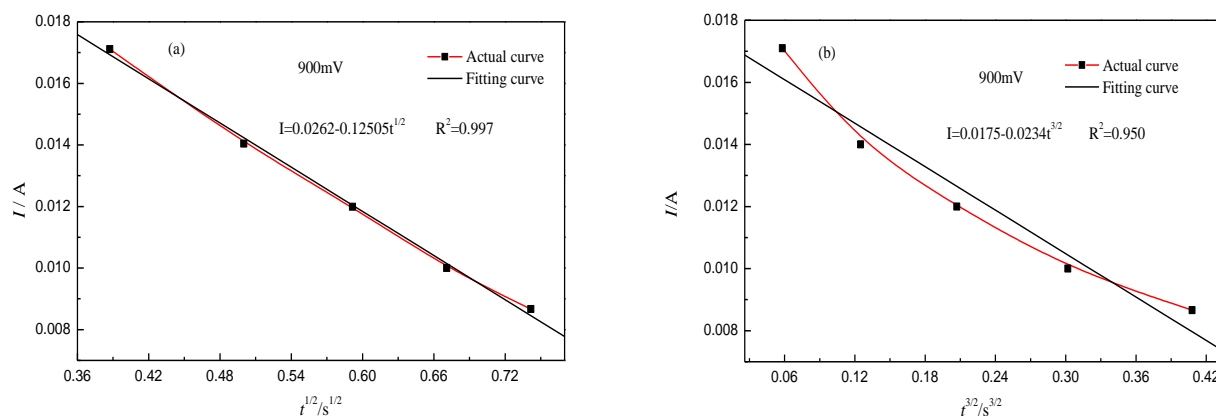


Figure 7. I vs. $t^{1/2}$ and I vs. $t^{3/2}$ plots for 900 mV chronoamperogram in Figure 6

3.3 Preparation and Characterization of V-Fe Gradient Materials

An electrodeposition experiment was carried out at 973 K for a molten salt system (composition: $X_{NaCl}=0.4; X_{KCl}=0.4; X_{NaF}=0.2$; and $X_{V_2O_3}=0.01$) using graphite as the anode and carbon steel as the cathode. A bi-directional pulse electrodeposition process was used. The current density was $200 \text{ mA}\cdot\text{cm}^{-2}$ for an electrodeposition time of 60 min. Figure 8 shows the surface morphology and local characteristics of the deposited samples under the experimental conditions, and the corresponding energy spectra. Little difference can be observed between the swept surface

morphology and the local energy spectrum of the deposited layer, and the surface of the deposited layer is compact and uniform with flat, fine grains. The surface elements are primarily vanadium (approximately 80%) and Fe (approximately 20%).

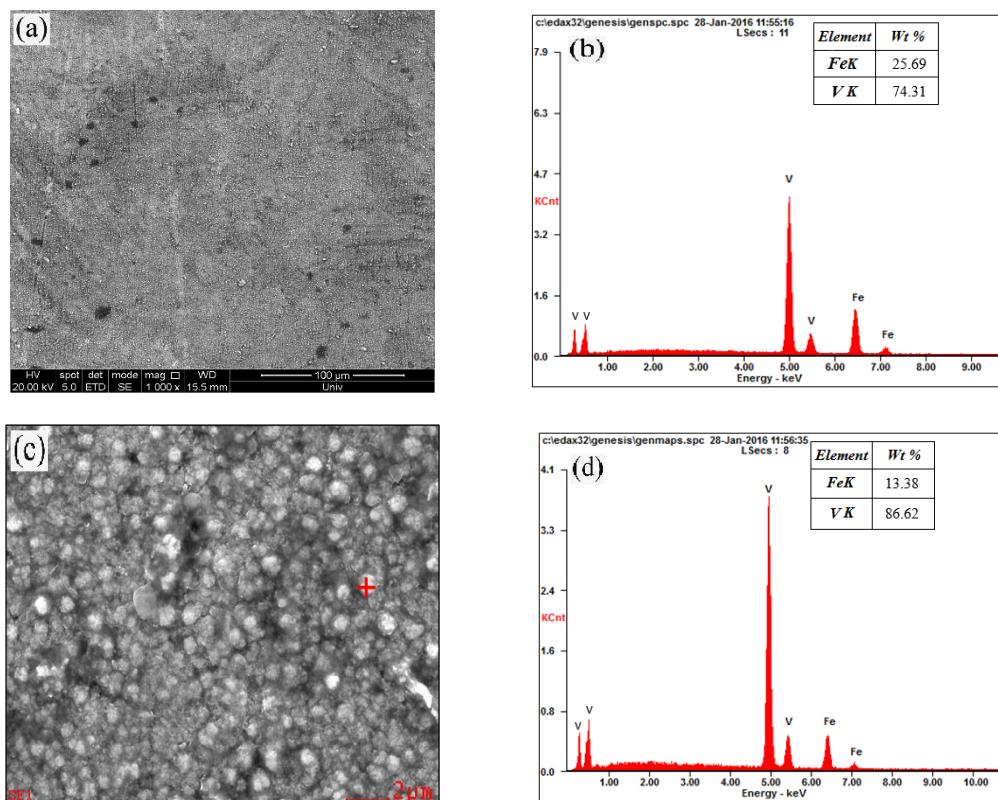


Figure 8. SEM image and EDS spectra of deposition layer surface and local area under experimental conditions

Fig. 9 shows the detection and analysis results for the coating surface using an optical microscope and a field emission scanning electron microscope. Fig. 10 shows the distribution of V and Fe contents over the sample cross-section as a function of the sample depth obtained using a GDA750 glow discharge spectrometer. Fig. 9 shows that the vanadium atoms in the coating are interdiffused with the iron atoms in the cathode carbon steel, where the V and Fe concentrations exhibit a gradient distribution, and the coating thickness is approximately 5.327 μm . From the coating surface to the carbon steel substrate, the vanadium content decreases gradually and the iron content increases. Li et al. obtained a similar result for the preparation of a Fe-Si alloy by electrodepositing silicon on carbon steel [20]. Fig. 10 shows that there is little difference between the coating thickness of the V-Fe gradient material and the result of the cross-section analysis, as the gradient layer is approximately 5- μm thick, and there is no pure V layer in the coating. Thus, the diffusion rate of V atoms in carbon steel exceeds the deposition rate of V atoms in carbon steel. The V-Fe phase diagram shows that V-Fe can form a solid solution under the experimental conditions. In this experiment, the V-Fe gradient layer is thin. This result is obtained because graphite is used as the anode material in

the experiment. In the electrodeposition process, the V_2O_3 concentration in the molten salt decreases over the course of the experiment and cannot be supplemented. To obtain a thick, pure V-Fe gradient layer, a V sheet should be used as the anode.

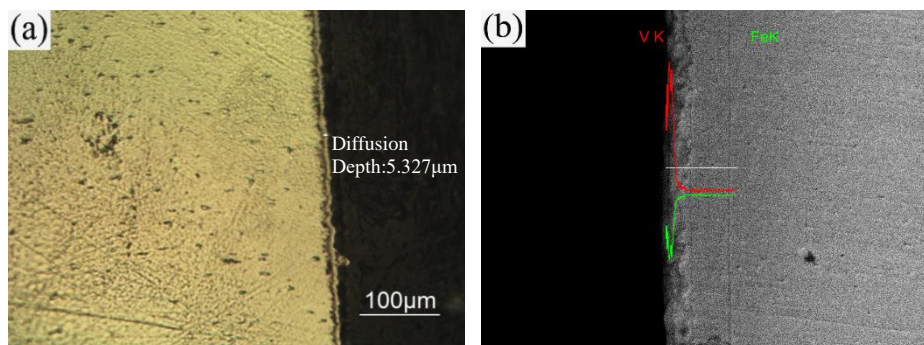


Figure 9. Appearance and EDS of section

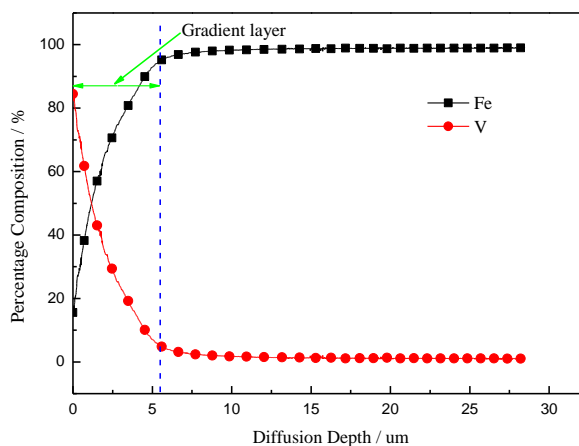


Figure 10. Distribution of V and Fe contents in sample section as a function of sample depth

5. CONCLUSIONS

The electrochemical reduction mechanism of V_2O_3 and the electrocrystallization process of V were studied in the molten salt system of NaCl-KCl-NaF- V_2O_3 at 973 K. Dense, uniform, flat and fine grains of V-Fe gradient materials were prepared on a carbon steel substrate. The thickness of the coating is approximately 5 μm . The results show that the electrochemical reduction process of V_2O_3 is a quasi-reversible process that is mix-controlled by the V^{3+} diffusion rate and the electron transport rate, The inverse reduction equation is $V^{3+} + 3e^- = 3V$, and the V^{3+} diffusion coefficient is 1.03×10^{-4} . The electrocrystallization process of V is an instantaneous hemispheroid three-dimensional nucleation process. Under the experimental conditions, V-Fe gradient materials form via the interdiffusion of vanadium and iron into an alloy layer.

ACKNOWLEDGEMENTS

This study was financially supported by the National Natural Science Foundation of China (Project No. 51474088).

References

1. D. L. Smith, H. M. Chung, H. Matsui, A. F. Rowcliffe, *Fusion Eng. Des.*, 41 (1998) 7.
2. J. H. Zhang, W. Zhang, L. Zhang, S. Q. Gu, *Int. J. Miner. Process*, 138 (2015) 20.
3. N. Ekmekci, İ. Keskin, *Metall. Mater. Trans. B.*, 20 (2019) 98.
4. Y. W. Zhao, Y. J. Wang, T. Q. Zhang, Y. Zhou, D. Zhang, *Rare Met. Mater. Eng.*, 38 (2009) 143.
5. R. Teghil, L. D'Alessio, V. Marotta, A. Santagata, G. De Maria, D. Ferro, M.A. Sansone, *Appl. Surf. Sci.*, 119 (1997) 34.
6. A. Kalkanli, E. E. Oren, *Powder Metall.*, 46 (2003) 324.
7. Z. Y. Cai, Y. G. Li, X. F. He, J. L. Liang, *Mater. Trans. B.*, 41 (2010) 1033.
8. S. X. Zhang, Y.G. Li, C. Wang, X. P. Zhao, *Int. J. Electrochem. Sci.*, 14 (2019) 91.
9. H. Li, J. L. Liang, S. S. Xie, R. G. Reddy, L. Q. Wang, *High Temp. Mater. Processes (London)*, 37 (2018) 921.
10. S. X. Zhang, Y. G. Li, K. Hu, X. P. Zhao, H. Li, J. L. Liang, *Int. J. Electrochem. Sci.*, 13 (2018) 8030.
11. Z. W. Tian, *Electrochemical method*, Science Publishing Company, (1984) Beijing (in Chinese).
12. J. Li, X. Y. Zhang, Y. B. Liu, Y. G. Li, R. P. Liu, *Rare Met.*, 005 (2013) 512.
13. J. Li, Y. G. Li, L. M. Liu, Z. Y. Cai, X. Y. Zhang, R. P. Liu, *Rare Met. Mater. Eng.*, 42 (2013) 2237.
14. Y. G. Li, J. Li, K. Zhang, L. M. Liu, *Acta Metall. Sin. (Engl. Lett.)*, 24 (2011) 466.
15. Y. F. Qi, *Basic research on the preparation of W-Cu FGM by electrodeposition (4)*, Hebei United University, (2014) Tangshan (in Chinese).
16. A. K. Shukla, B. Hariprakash, *Encyclopedia of Electrochemical Power Sources*, Elsevier Science Publishing Co. Inc, (2009) Netherlands.
17. X. Shu, Y. Y. Wang, C. M. Liu, A. Aljaafari, W. Gao, *Surf. Coat. Tech.*, 261 (2015)
18. Y. K. Gu, J. Liu, S. X. Qu, Y. D. Deng, X. P. Han, W. B. Hu, C. Zhong, *J. Alloy. Compd.*, 690 (2017) 228.
19. J. L. Liang, H. Li, D. X. Huo, H. Y. Yan, R. G. Reddy, L. G. Wang, L. Q. Wang, *Ionics.*, 24 (2018) 3221.
20. H. Li, D. B. Wang, J. L. Liang, H. Y. Yan, Z. Y. Cai, R. G. Reddy, *Int. J. Chem. React. Eng.*, 18 (2019) 1542.